MICROSTRUCTURAL ANALYSIS OF HOT ISOSTATICALLY PRESSED AL-SIC

Bronsveld, P.M.; Hosson, J.Th. De; Sargent, M.A.; Alsem, W.H.M.

Published in:
Materials science and engineering a-Structural materials properties microstructure and processing

DOI:
10.1016/0921-5093(91)90540-4

Publication date:
1991

Microstructural analysis of hot isostatically pressed Al-SiC

P. M. Bronsveld, P. Bruinsma and **J. Th. De Hosson**
Department of Applied Physics, Materials Science Centre, University of Groningen, Nijenborgh 18, 9747 AG Groningen (The Netherlands)

M. A. Sargent and **W. H. M. Alsem**
Billiton Research B.V., P.O. Box 38, 6800 LH Arnhem (The Netherlands)

Abstract

The difference between extruded and hot isostatically pressed (HIP) Al_{6061} both with a T6 final heat treatment and with a 30 wt.% SiC particulate reinforcement is one of densification. The higher density of the HIP material is not translated into a stronger material. The Mg_2Si precipitation is favoured by the presence of the SiC reinforcement in both samples. HIP powder metallurgy material reveals clearly the original powder particle boundaries, in contrast to the more smeared-out stringers in the extruded material. Cleavage of SiC particles by neighbouring SiC particles is observed in the HIP samples, making them less ductile.

1. Introduction

The main reason for mixing with SiC is the improvement of the mechanical properties of the aluminium alloy, which is itself already hardened by Mg_2Si precipitates.

In a recent NASA [1, 2] report on several aluminium matrix composites it was stated that the elastic moduli of the composites are found to be isotropic and independent of the type of reinforcement used. The yield and tensile strength and the ductility are controlled primarily by the matrix alloy, the temper condition and the reinforcement content. The type and orientation of the reinforcement had some effect on the yield and tensile strength of the composites, but only for those in which whiskers were more highly oriented. It could be concluded that particulate reinforcements are as effective as whisker reinforcement.

On the basis of these data for particulate-reinforced extruded material, we have plotted in Fig. 1 the Young's modulus and the fracture strain *vs.* the percentage reinforcement. The result is a linear increase in the Young's modulus, but at the same time an almost linear decrease in the fracture strain to a value below 1% at 30% reinforcement. To understand and improve on this result we have made a microstructural analysis of a hot isostatically pressed (HIP) Al_{6061} powder reinforced with 30 wt.% SiC particulates and given a final T6 heat treatment as described in a recent paper by Sargent *et al.* [3]. One of the problems the manufacturer is confronted with is the wettability of the constituents. Contact angle

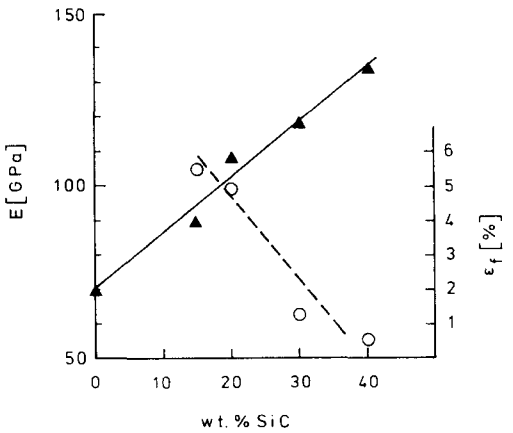

Fig. 1. Young's modulus and fracture strain *vs.* amount (weight per cent) of SiC particulates for extruded material [1, 2].

0921-5093/91/$3.50

measurements indicate that only at higher temperatures can a good wetting be achieved [4]. However, at the same time a reaction takes place between the aluminium matrix and the SiC particulates, resulting in the formation of Al_4C_3 and free silicon at the interface which diminishes the crack toughness properties. The reaction kinetics can be slowed down by alloying the matrix with silicon. The amount of silicon dissolved in the matrix can be determined by differential scanning calorimetry (DSC) measurements of the liquidus temperature of the matrix [5]. Magnesium addition promotes wetting of SiC by aluminium [6]. DSC measurements indicate that the mere presence of SiC favours the formation of Mg_2Si precipitates [7]. Al_{6061} and SiC powder particles only form sound interfacial bonds at high temperature. Cooling to ambient temperature introduces a hydrostatic tensile stress in the aluminium matrix of the order of 200 MPa [8].

2. Sample material and preparation

Different samples were analysed as provided by Billiton Research in the form of solid bars 10 mm in diameter. Crucial to the experiment was the preparation of the samples for the electron microscope [9]. Samples 3 mm in diameter and 0.5 mm thick were cut by spark erosion. Subsequently, they were thinned first by grinding and secondly by dimpling equally on both sides to a thickness of 20 μm using a GATAN dimpler. Then the samples were further thinned by a GATAN micro ion milling device with a 4 kV argon ion beam under an angle of 8°. Occasionally the samples were given a final electrochemical treatment in a TENUPOL instrument. It turned out to be necessary during the ion milling and electrochemical processing steps to check the sample from time to time by putting it into the microscope in order to see whether the SiC as well as the Al_{6061} were sufficiently transparent and also to make sure that we were not looking at artifacts introduced by the sample preparation methods. As electron microscope we used a JEOL 200 CX side entry machine with a high angle/selected area pole piece as an objective lens at an operating voltage of 120 kV.

3. Results

Microstructural scanning electron microscopy (SEM) analysis of HIP material revealed as a characteristic pattern the oxide traces of the original powder particle boundaries (PPBs). Those PPBs can best be found in unreinforced HIP samples. An example taken from sample 2 is depicted in Fig. 2. In extruded samples the oxide layers are smeared out to so-called stringers. Table 1 gives the mechanical data of extruded and HIP Al_{6061} without and with a reinforcement of 30 wt.% SiC. The HIP Al_{6061} reinforcement material is far less ductile than when extruded. The hydrostatic tensile stress in the aluminium matrix resulting from a large difference in coefficient of thermal expansion between matrix and reinforcement favours Mg_2Si precipitation in the matrix during the T6 heat treatment. This holds both for extruded and HIP material and should improve the mechanical properties equally. Six different samples were subsequently studied by transmission electron microscopy (TEM).

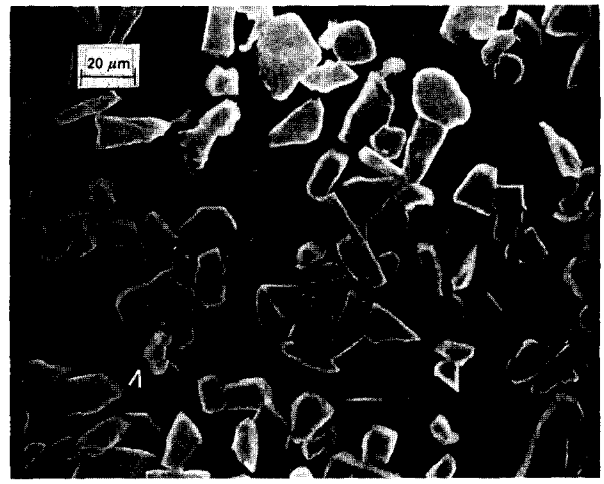

Fig. 2. SEM micrograph of sample 2. The arrow indicates a cleaved SiC particle. The original powder particle boundaries are undistorted.

TABLE 1

Comparison between extruded and hot isostatically pressed Al_{6061} without and with a 30 wt.% SiC reinforcement

	Al_{6061}		Al_{6061} + 30 wt.% SiC	
	Extruded	HIP	Extruded	HIP
$\sigma_{0.2}$ (MPa)	322	330	300	395
σ_{UTS} (MPa)	374	350	415	417
E (GPa)	72.8	72.3	112	117
ε_f (%)	10.9	10.1	2.8	0.7
ρ (g cm^{-3})	2.599	2.700	2.763	2.835

3.1. Sample 1: Al_{6061} + 30% SiC; hot isostatically pressed for 3 h (canned), T6

A dense network of Mg_2Si needles along ⟨100⟩ directions was observed. Two types of boundaries were observed. Along the normal grain boundaries we observed large heterogeneously formed Mg_2Si precipitates together with precipitate-free zones on both sides of them. Occasionally a wide band of differently looking particles could be found as shown in Fig. 3. They were interpreted as being a small section of a PPB. The original particles are 25 μm in diameter and only a small section of 5 μm shows up on a micrograph such as Fig. 3.

3.2. Sample 2: Al_{6061} + 30% SiC; hot isostatically pressed for 3 h (canned), hot isostatically pressed for 3 h (uncanned), T6

An additional "uncanned" HIP treatment has made the Mg_2Si needle network even denser. The precipitate-free zones are reduced in size. No reaction layer has been formed yet. The high UTS of 417 MPa can be well understood from this microstructure. A dark field TEM micrograph is reproduced in Fig. 4. The beam was parallel to the [001] direction. In such a case the Mg_2Si precipitates, aligned along ⟨100⟩ directions, are projected under a 90° angle. Dislocations are severely hindered when moving through such a maze pattern of needles.

3.3. Sample 3: Al_{6061}; hot isostatically pressed for 1 h (canned), T6

Mg_2Si precipitates are visible as small dots with a slight tendency to align themselves along ⟨100⟩ directions. They are not as fully grown as the needles depicted for sample 1 although both samples had a T6 heat treatment as the final processing step. A possible reason is the shorter HIP time (1 h instead of 3 h). Another possibility is the absence of SiC particulates. The large difference in coefficient of thermal expansion of these particulates with respect to the aluminium matrix causes a tensile stress, extra dislocations and an excess number of thermal vacancies to be introduced during the cooling cycle of the HIP treatment and they may stimulate the precipitation [7]. Grain boundaries could be imaged rather easily but the imaging of dislocations was hampered by the preferred precipitation on them.

3.4. Sample 4: Al_{6061}; hot isostatically pressed for 1 h (canned), hot isostatically pressed for 3 h (uncanned), T6

In Fig. 5 Mg_2Si precipitates are clearly visible as dots with a strong tendency to align themselves

Fig. 4. TEM micrograph of sample 2. Full-grown Mg_2Si needles along ⟨100⟩ directions.

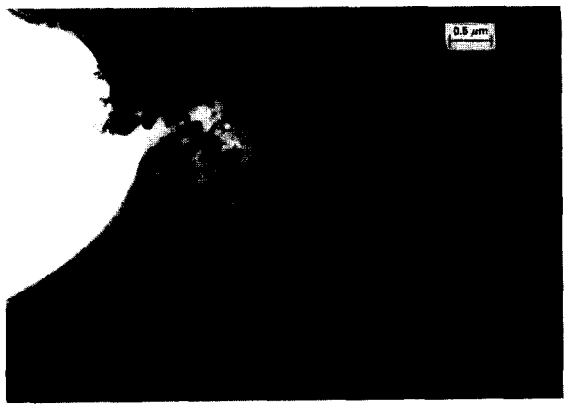

Fig. 3. TEM micrograph of sample 1. An enlarged view of an original PPB.

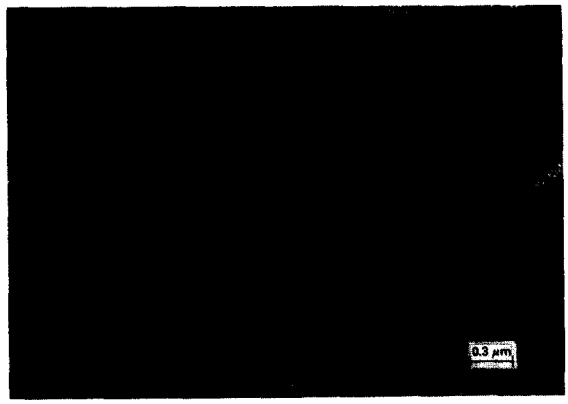

Fig. 5. TEM micrograph of sample 4. The Mg_2Si precipitates are underdeveloped in comparison with those in Fig. 4.

along ⟨100⟩ directions. Even now the T6 treatment has not produced the Mg_2Si needles as observed in sample 1 so the effect of the SiC particulates is definitely present. From a comparison between the precipitate-free zones in samples 2 and 4 it could be concluded that the density of precipitates is much higher in sample 2 than in sample 4. High concentrations of large precipitates are visible, located at the original PPBs.

3.5. Sample 5: Al_{6061} + 30% SiC; hot isostatically pressed for 3 h (canned)

The absence of Mg_2Si precipitates made TEM imaging of dislocations and reaction layer easy. The reaction layer is almost non-existent. The large amount of plastic deformation in several SiC particulates, invoked partly by neighbouring SiC particulates as already observed by Withers *et al.* [9] or, otherwise, as a secondary effect of an earlier processing step, should be noted.

3.6. Sample 6: Al_{6061} + 30% SiC; hot isostatically pressed for 3 h (canned), solution heat treatment, T6

Mg_2Si precipitates are visible as dots in the matrix. Dislocations seem to originate from the matrix–SiC interface as was observed in a TEM heating stage during cooling.

4. Discussion

A large number of papers with experimental data and model explanations have recently been published. Two basic papers should be mentioned here, that by Eshelby [10] giving a description of the stress field of a foreign inclusion in a matrix with different elastic constants and that by Ashby [11] about the deformation of plastically non-homogeneous materials. In the former case the stress components are the crucial parameters; in the latter case geometrically necessary dislocations play an important role. It is useful to realize that, if one looks at the r dependence, the stress component around an inclusion is proportional to r^{-3} while dislocations have a field of influence proportional to r^{-1}. In our microanalysis we have observed a number of dislocations, but there is no evidence that they play a dominant role during the processing steps. More information with respect to the effects of dislocations can be found in a paper by Arsenault and his group [12]. The tensile stress introduced in the matrix by the SiC particles which was measured by Ledbetter and Austin [8] as being +200 MPa causes a more fully grown Mg_2Si precipitate network. When in solution in aluminium, magnesium and silicon tend to cluster together to form the f.c.c. phase of Mg_2Si with a lattice parameter which is considerably larger than that for aluminium. A tensile stress may favour such a behaviour. A nice example of the influence of the stress field around a particle on precipitation behaviour can be found in a paper by Sato *et al.* [13] in a monocrystalline Fe–N matrix.

Concerning decohesion of the SiC–Al interface *vs.* cleavage of individual particulates Sargent *et al.* [3] observed a considerable number of failure surfaces in the SiC particulates embedded in a ductile matrix. For both extruded and HIP samples the interfaces seem to be of proper quality. Withers *et al.* [9] have studied the interface between aluminium and SiC with high resolution electron microscopy and they came to the conclusion that only a 2 nm thin amorphous layer exists. However, it is not yet obvious whether this layer is good or bad for the strength of the metal matrix composite. Cleavage of the SiC particulates may occur, especially because nearby particulates can act as stress raisers (Fig. 6). This explains the dramatic fall in strain at fracture with the amount of reinforcement given in Fig. 1. Nutt [14] reports evidence of the initiation and growth of voids at locations of high stress around the SiC particulates. This is made more explicit by a recent finite element study by Levy and Papazian [15]. Our TEM results did not reveal these voids. It is important therefore to

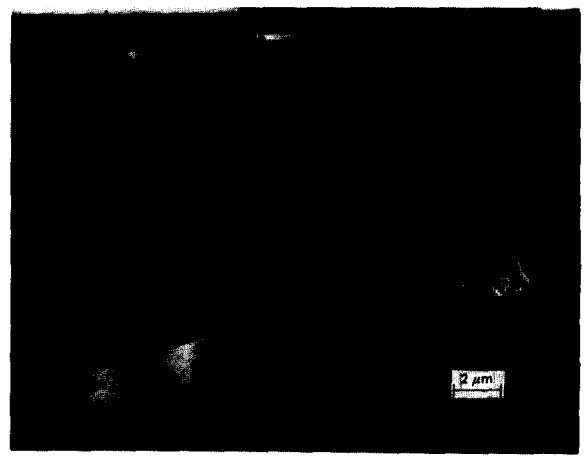

Fig. 6. TEM micrograph of sample 5. An SiC particle is severely damaged by a neighbouring SiC particle.

continue this study and especially to compare the interface in HIP and extruded Al–SiC with high resolution electron microscopy.

4. Conclusion

The difference between extruded and HIP material was a 2.5% higher degree of densification for the latter processing step. This difference did not result in an improvement in UTS for the HIP samples. TEM results did not reveal void formation around SiC particulates in either of the samples but they did indicate severe deformation of SiC particulates by neighbouring particulates in the HIP samples. This caused a reduction in strain at fracture for these samples from 2.8% to 0.7%.

References

1 D. L. McDanels and C. A. Hoffman, Microstructure and orientation effects on properties of discontinuous silicon carbide/aluminum composites, *NASA Tech. Pap. 2302*, 1984 (National Aeronautics and Space Administration).

2 D. L. McDanels, Analysis of stress–strain, fracture and ductility behaviour of aluminum matrix composites containing discontinuous silicon carbide reinforcement, *Metall. Trans. A, 16* (1985) 1105.

3 M. A. Sargent, C. Rensen and W. H. M. Alsem, The structure and properties of particulate-SiC/aluminum alloy 6061 metal-matrix composite manufactured via hot isostatic pressing. In R. B. Bhagat, A. H. Clauer, P. Kumar and A. M. Ritter (eds.), *Metal and Ceramic Composites: Processing, Modelling and Mechanical Behavior*, Minerals, Metals and Materials Society, Warrendale, PA, 1990.

4 M. Shimbo, N. Naka and I. Okamoto, Wettability of silicon carbide by aluminium, copper and silver, *J. Mater. Sci. Lett., 8* (1989) 663.

5 D. J. Lloyd and I. Jin, A method of assessing the reactivity between SiC and molten Al, *Metall. Trans. A, 19* (1988) 3107.

6 S.-Y. Oh, J. A. Cornie and K. C. Russell, Wetting of ceramic particulates with liquid aluminum alloys: part II. Study of wettability, *Metall. Trans. A, 20* (1989) 533.

7 J. M. Papazian, Effects of SiC whiskers and particles on precipitation in aluminum matrix composites, *Metall. Trans. A, 19* (1988) 2945.

8 H. M. Ledbetter and M. W. Austin, Internal strain (stress) in an SiC–Al particle-reinforced composite: an X-ray diffraction study, *Mater. Sci. Eng., 89* (1987) 53.

9 P. J. Withers, W. M. Stobbs and A. J. Bourdillon, Various TEM methods for the study of metal matrix composites, *J. Microsc., 151* (1988) 159.

10 J. D. Eshelby, The continuum theory of lattice defects, *Solid State Phys., 3* (1956) 79.

11 M. F. Ashby, The deformation of plastically non-homogeneous materials, *Philos. Mag., 21* (1970) 399.

12 R. J. Arsenault and N. Shi, Dislocation generation due to differences between the coefficients of thermal expansion, *Mater. Sci. Eng., 81* (1986) 175.

13 A. Sato, T. Mor and Y. Tanaka, Stress distribution around an inclusion in an Fe–N single crystal, *Acta Metall., 27* (1979) 131.

14 S. R. Nutt, Interfaces and failure mechanisms in Al–SiC composites. In A. K. Dhingra and S. G. Fishman (eds.), *Interfaces in Metal-Matrix Composites*, Metallurgical Society of AIME, Warrendale, PA, 1986.

15 A. Levy and J. M. Papazian, Tensile properties of short fiber-reinforced SiC/Al composites: part II. Finite-element analysis, *Metall. Trans., 21* (1990) 411.